Journal of Electroceramics, 14, 255–264, 2005

Partial Electronic Conductivity and Chemical Diffusivity of $Li_{3x}La_{2/3-x}TiO_3$ Solid Solution

LIAN-XING HE, DOH-KWON LEE & HAN-ILL YOO*

Solid State Ionics Research Lab., School of Material Science and Engineering, Seoul National University, Seoul 151-742, Korea

Submitted August 18, 2004; Revised December 23, 2004; Accepted December 28, 2004

Abstract. Partial electronic conductivity and chemical diffusivity of Li have been measured on the system of $Li_{3x}La_{2/3-x}TiO_3$ (LLT) with $x = 0.13$, a prospective Li^+ electrolyte, against oxygen activity in the range of $10^{-22} < a_{O_2} < 0.21$ at 557°, 610° and 663°C, respectively by an ion-blocking polarization technique. It is found that the electronic conductivity of LLT, which in air is essentially an ionic conductor, varies as $a_{O_2}^{-1/4}$ to render it mixed-conductive in reducing atmospheres, say, in $a_{O_2} < 10^{-12}$. The chemical diffusivity of component Li also increases from a value of the order of 10^{-8} cm^2/s in air atmosphere up to a maximum on the order of 10^{-3} cm^2/s as the electronic conductivity increases with decreasing oxygen activity. This is attributed to the variation of the electronic transference number and the thermodynamic factor with oxygen activity. The latter has been evaluated to be on the order of 10–10^3.

Keywords: $Li_{3x}La_{2/3-x}TiO_3$, partial electronic conductivity, chemical diffusivity, polarization technique

1. Introduction

Since Belous et al. [1] and Inaguma et al. [2] reported on the exciting discovery of unusually high lithium ion conductivity in titanate-based solid solutions $Li_{3x}La_{2/3-x}TiO_3$ (LLT) with a perovskite-related structure, these materials have received a considerable attention due to their potential use as an electrolyte for solid state ionic devices such as secondary batteries, chemical sensors and electrochromic displays. Naturally most of the related works have been focused on the characterization, understanding or improvement of their ionic conductivity [3–14]. Their partial electronic conductivity is also an important property to characterize particularly against Li-activity for their application as electrolytes. Actually, one drawback of LLT is known to be the fact that they tend to be reduced at high Li-activity and increase the partial electronic conductivity [2]. To the best of our knowledge, nevertheless, no systematic study has yet been done on their electronic conductivity.

*To whom all correspondence should be addressed. E-mail: hiyoo@plaza.snu.ac.kr

We have investigated the partial electronic conductivity along with the chemical diffusivity on a system of LLT against oxygen activity by a Hebb-Wagner polarization technique [15–17]. The oxygen activity, instead of Li-activity, was chosen as the experimental variable because it is much easier to control experimentally. Furthermore, a spatial variation or difference of oxygen activity may be regarded as a measure of that of Li-activity in the system LLT as the rest components La, Ti and O are practically immobile to remain spatially uniform in distribution [18]. In this paper, we will report the partial electronic conductivity and chemical diffusivity of LLT as a function of oxygen activity in the range of $10^{-22} < a_{O_2} < 0.21$ at 557°, 610° and 663°C, respectively.

2. Theoretical Background

Since the initiative works by Hebb [15] and Wagner [16], polarization of a mixed conductor in a semi-blocking cell has widely been used to study the partial electronic conductivity of mostly ionic conductor

materials. The transient solutions have earlier been available to the polarization or depolarization process only under galvanostatic boundary conditions [19–21]. Recently, Lee and Yoo [17] have proposed more general transient solutions for the polarization and relaxation processes under not only galvanostatic, but also potentiostatic boundary conditions even in the presence of the interference effect between electrons and ions.

High ionic conductivity of the present system LLT is attributed to the presence of abundant vacancies and Li^+ ion in the A-sublattice of the perovskite structure ABO_3 [22]. One may, thus, reasonably assume that component La, Ti and O are essentially immobile at the temperatures of present interest, and consider Li^+ cations and electrons to be the mobile charged components of the system.

When the electrochemical perturbation leading to a chemical polarization is small enough, the partial ionic and electronic conductivities of the system, σ_{Li^+} and σ_e, respectively, may be regarded as constant. The chemical polarization and depolarization processes can then be described in terms of μ_{Li}, the chemical potential of chemical component Li by a simple chemical diffusion process[1] [17]:

$$\frac{\partial \mu_{Li}}{\partial t} = \tilde{D}\nabla^2 \mu_{Li} \tag{1}$$

with the chemical diffusivity, $\tilde{D}$ defined in accord with Wagner [23, 24] as

$$\tilde{D} = \frac{RT}{F^2}\frac{\sigma_{Li^+} t_e}{c_{Li}}\left(\frac{\partial \ln a_{Li}}{\partial \ln c_{Li}}\right) \tag{2}$$

where t_e is the electronic transference number, a_{Li} and c_{Li} the activity and concentration, respectively, of the chemical component Li, and others have their usual significance.

For a polarization process, the initial condition is taken as a uniform distribution of Li or uniform chemical potential μ^*_{Li}:

$$\mu_{Li} = \mu^*_{Li} \quad \text{at } 0 < x < L \tag{3}$$

where L denotes the length of the specimen. The boundary conditions are determined by the polarization mode employed [17]: For a galvanostatic ion-blocking mode which will be employed in experiment later on, they are

$$J_{Li^+}(x, t) = 0 \quad \text{at } x = 0, L \tag{4}$$

$$J_e(x, t) = -i^o/F \quad \text{at } x = 0, L \tag{5}$$

associated with the flux equations for Li^+ and electrons

$$J_{Li^+} = -\frac{\sigma_{Li^+}}{F^2}\nabla \eta_{Li^+} \tag{6}$$

$$J_e = -\frac{\sigma_e}{F^2}\nabla \eta_e \tag{7}$$

and the local equilibrium criterion,

$$\nabla \mu_{Li} = \nabla \eta_{Li^+} + \nabla \eta_e \tag{8}$$

where i^0 is a constant current density passed and $\nabla \eta_k$ the electrochemical potential gradient of charged mobile component of k-type.

The transient solution to Eq. (1) takes the form [17]

$$\mu_{Li}(\xi, \omega) = \mu^*_{Li} + \frac{i^0 FL}{\sigma_e}\left[\left(\xi - \frac{1}{2}\right) + \Theta(\xi, \omega)\right] \tag{9}$$

with

$$\Theta(\xi, \omega) \equiv \frac{4}{\pi^2}\sum_{n=1}^{\infty}\frac{1}{(2n-1)^2}\cos\{(2n-1)\pi\xi\} \times \exp\{-(2n-1)^2\omega\}; \quad \xi \equiv \frac{x}{L}$$

$$\omega \equiv \frac{t}{\tau} = \frac{\tilde{D}\pi^2 t}{L^2}. \tag{10}$$

For the depolarization process from a steady state polarization, on the other hand, the initial condition is the steady state distribution resulting from the polarization process [Eq. (9) as $\omega \to \infty$] and the boundary conditions are

$$\begin{aligned} J_{Li^+}(x, t) &= 0 \quad \text{at } x = 0, L \\ J_e(x, t) &= 0 \quad \text{at } x = 0, L \end{aligned} \tag{11}$$

The transient solution then takes the form [17]

$$\mu_{Li}(\xi, \omega) = \mu^*_{Li} - \frac{i^0 FL}{\sigma_e}\Theta(\xi, \omega) \tag{12}$$

One may monitor the polarization or depolarization by measuring the difference of electronic electrochemical potential $\Delta\eta_e$ or voltage drop $\Delta V_e (= -\Delta\eta_e/F)$ between two potential probes that are appropriately located along the specimen length. The electronic electrochemical potential difference is related to the

chemical potential distribution due to Eqs. (6)–(8) as [17],

$$\nabla\eta_e = \frac{i^o F}{\sigma} + t_{\mathrm{Li}^+}\nabla\mu_{\mathrm{Li}} \tag{13}$$

where t_{Li^+} is the transference number of Li^+ ions.

If the two potential probes are positioned symmetrically with respect to the center of a bar specimen ($\xi = 1/2$) with a separation distance $\Delta\xi$, then it can be easily shown [17] that

$$\Delta V_e = i^o L\left[\frac{\Delta\xi}{\sigma_e} - \frac{2t_{\mathrm{Li}^+}}{\sigma_e}\Theta\left(\frac{1-\Delta\xi}{2}, \omega\right)\right] \tag{14}$$

during polarization, and

$$\Delta V_e = -i^o L\frac{2t_{\mathrm{Li}^+}}{\sigma_e}\Theta\left(\frac{1-\Delta\xi}{2}, \omega\right) \tag{15}$$

during depolarization. Obviously, the initial voltage drops are, respectively,

$$\Delta V_{e,0} = t_e\frac{i^o L\Delta\xi}{\sigma_e}; \quad \Delta V_{e,0} = t_{\mathrm{Li}^+}\frac{i^o L\Delta\xi}{\sigma_e} \tag{16}$$

As $t \to \infty$, on the other hand, Eq. (14) approaches the steady state polarization potential or

$$\Delta V_{e,\infty} = \frac{i^0 L\Delta\xi}{\sigma_e}. \tag{17}$$

3. Experimental

Reagents of Li_2CO_3(4N, Aesar, USA), La_2O_3(3N, Aldrich Chemical Company Inc., USA) and TiO_2(3N, Aldrich Chemical Company Inc., USA) were used as the starting materials. Due to its hygroscopicity, La_2O_3 was fired at 900°C for 6 h to remove water and/or carbon dioxide prior to weighing. A stoichiometric mixture of these powders, corresponding to the lattice molecular formula $Li_{3x}La_{2/3-x}TiO_3(x = 0.13)$, was heated at 800°C for 3 h to drive off CO_2. After grinding, the mixture was calcined at 1000°C for 12 h. Then, the calcined powder was ground, and pressed into pellets of 10 mm diameter and 2–4 mm thickness under the pressure of 150 MPa, which were subsequently sintered at the temperature of 1150–1300°C for 6 h, embedded in the powder of the same composition to suppress lithium loss. Identification of the crystalline phase of the sintered specimens was later carried out by powder X-ray diffractometry (XRD).

The as-sintered sample, with a density higher than 95% of the theoretical one, were cut with a low speed saw into parallelepipeds measuring (1–1.4) mm × (1–1.4) mm × 9 mm. The ion-blocking electrodes were prepared by sputtering Pt about one μm thick onto the both ends of a parallelepiped specimen. As the inner potential probes, two Pt wires of 0.2 mm diameter were wound around 2–3 mm apart ($= L\Delta\xi$ in Eq. (14) or (15)) equidistant from the center of a specimen. In order to secure a good electrical contact with the inner probes, a little platinum paste was applied to the surface of the Pt wires and then they were wound tight through the grooves which had earlier been made 0.25 mm wide and 0.3 mm deep along a longitudinal edge of the specimen. The as-prepared ion-blocking cell is schematically illustrated in Fig. 1.

The oxygen activity in the surrounding was controlled by N_2/O_2 or CO/CO_2 gas mixtures, and monitored by a zirconia-based oxygen sensor.

When the specimen was fully equilibrated in a fixed oxygen activity atmosphere, a constant current was passed via the sputtered Pt-electrodes by using a current source (Keithley 220), and the potential drop, ΔV_e, between the inner probes was monitored using an electrometer (Keithley 196) which was interfaced with a personal computer. The current was chosen in such a way that the applied voltages be low enough (less than 100 mV) not to electrolyze lithium out.

The transient voltage drops as measured were finally fitted to Eq. (14) [or (15) for comparison] to evaluate $\Delta V_{e,\infty}$ (Eq. (17)), τ (Eq. (10)) and t_{Li^+}as the fitting parameters and from the first two parameters, in turn, σ_e and $\tilde{D}$ were determined. It has turned out that as long as a polarization process is closely monitored long enough (so that the corresponding steady state is incipient at least), the first two can be generally determined precisely enough. To the contrary, the last is sensitive to a few data in the very beginning or how fast the data are acquired (because it is actually determined by the

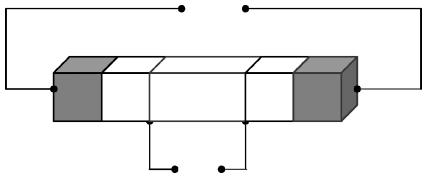

Fig. 1. Schematic of an electrochemical cell with ion-blocking electrodes.

initial voltage jump, $\Delta V_{e,0}$, Eq. (16)) and hence, the evaluated $t_{Li^+}$is normally subjected to a considerable uncertainty.

4. Results and Discussion

4.1. Phase Purity

For the nominal composition of $Li_{3x}La_{2/3-x}TiO_3 (x < 1/6)$, different space groups are found in literature depending on the degree of reliability of the XRD result refinement [2, 10, 12, 25, 26]. The XRD pattern of our as-sintered LLT sample is as shown in Fig. 2. Besides the major peaks for the cubic perovskite cell are observed two types of superstructure reflection lines: (a) the ordering of La and Li or vacancy along the doubled *c*-axis (in triangle); (b) ordering of La, Li and vacancies with a rocksalt arrangement (in closed circle). No appreciable impurity phase is observed within the resolution of the XRD employed and hence, the present specimens may be regarded as an X-raywise pure cubic phase.

4.2. Transient Voltage Drop

Figure 3(a) and (b) show the typical polarization and/or depolarization behavior in air and in a far reduced atmosphere of $\log a_{O_2} = -18.8$, respectively. It is noted that polarization kinetics is extremely sluggish in air atmosphere in contrast to that in far reduced atmospheres. This is why the depolarization step could not be successfully monitored in the air. One can clearly see in Fig. 3(b) that as described by Eqs. (14) and (15), an initial voltage drop (Eq. (15)) is followed by an exponential saturation during polarization and that (Eq. (15)) by an exponential decay during relaxation. The time variations of the voltage drops are quite satisfactorily fitted to Eqs. (14) or (15) as depicted by the solid lines in Fig. 3.

Theoretically, the voltage jumps (or IR drops) immediately after switching on or switching off the current should correspond to the total conductivity of the specimen. As is seen, the part of "IR drop" in Fig. 3(a) is too small even to discern an "obvious" jump. This indicates that the total conductivity of the specimen LLT is much larger than the partial electronic conductivity and hence, a predominantly ionic conductor in air. In the far reduced atmosphere (Fig. 3(b)), on the other hand, the part of "IR drop" was appreciably increased to become comparable with the stationary value. It indicates that the LLT has now become a mixed ionic electronic conductor ($t_e \approx 0.7$). Nevertheless, the total conductivities as determined from the initial voltage jumps are often not so reliable because the voltage value extrapolated to the moment of switching-on or switching-off is normally subjected to a considerable error due to the limited data acquisition rate of a measuring instrument employed. In such a case, the AC Impedance Spectroscopy (IS) technique is often used

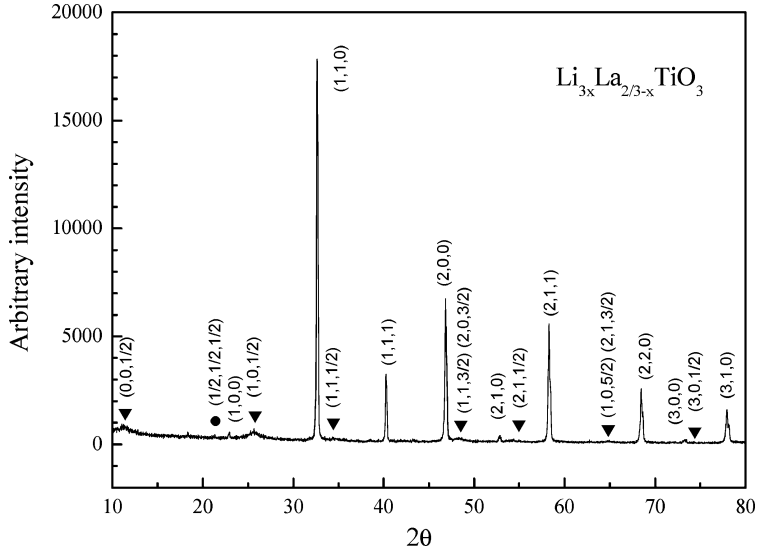

Fig. 2. Typical XRD patterns of LLT.

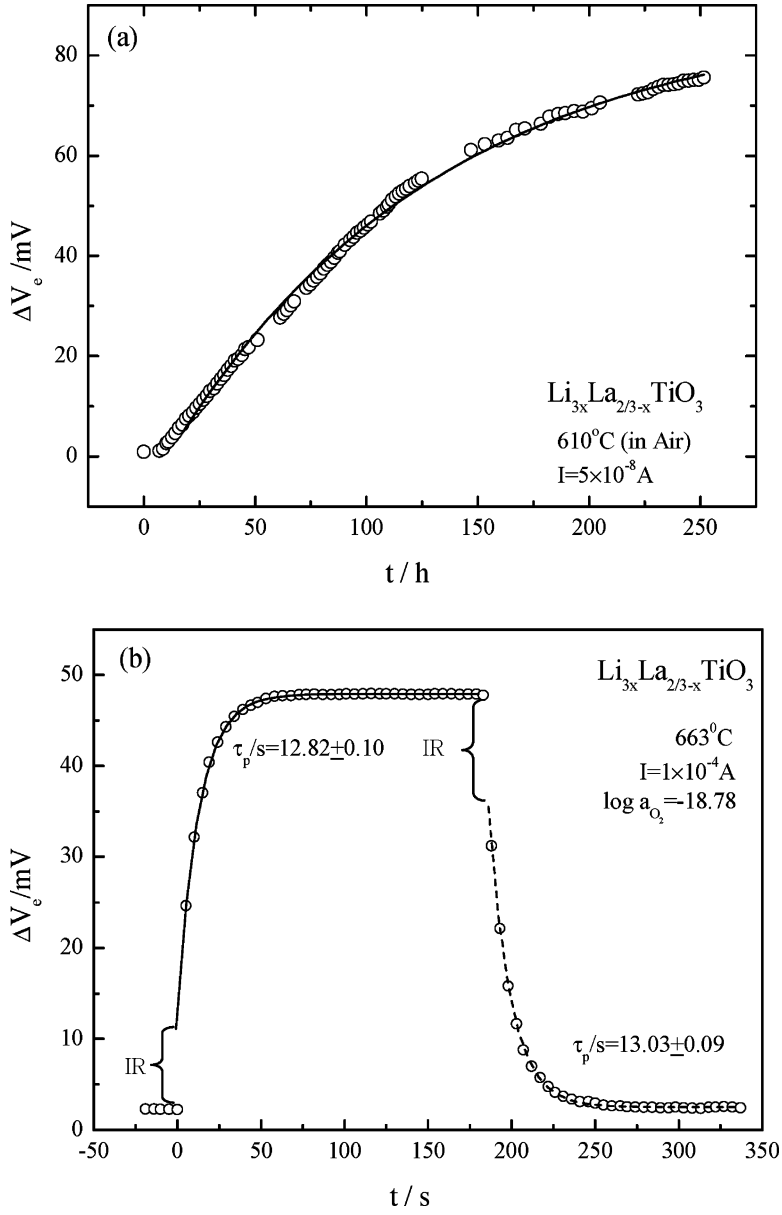

Fig. 3. Typical voltage response under galvanostatic conditions: (a) 610°C, $\log a_{O_2} = -0.68$; (b) 663°C, $\log a_{O_2} = -18.78$. The solid and dashed lines are the best-fitted to Eq. (14) and (15), respectively.

as a good complement to get more accurate σ_{tot}. Unfortunately, however, the present specimen LLT is too conductive at the temperatures of present concern and hence, it was neither trivial to get the total conductivity values precisely enough by the impedance spectroscopy, especially under the far reduced atmosphere.

The temporal variations of voltage drop of the LLT specimen under different atmospheres are compared in Fig. 4, where the fitted values for τ are also listed. It is seen that the relaxation times are all on the same order of magnitude, but exhibiting a minimum, which will be considered later on.

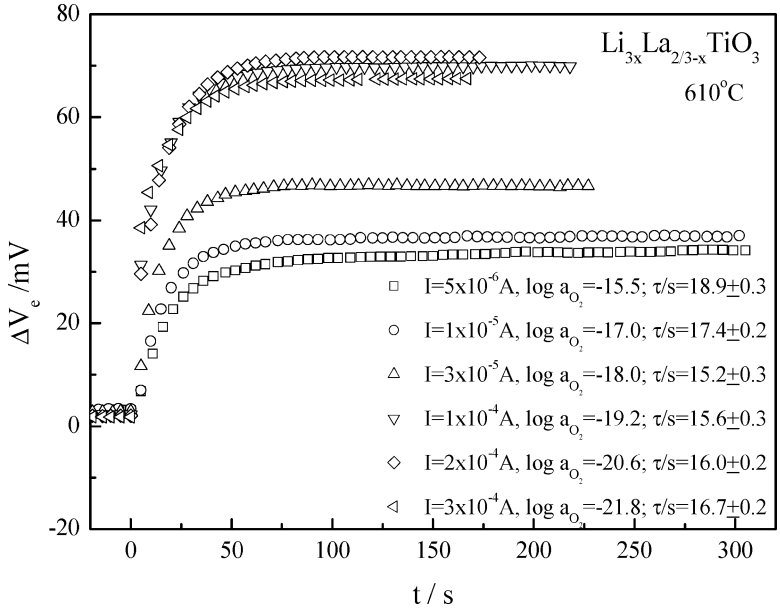

Fig. 4. Temporal variation of the voltage drop across the ion-blocking cell of Fig. 1 at different atmospheres at a fixed temperature.

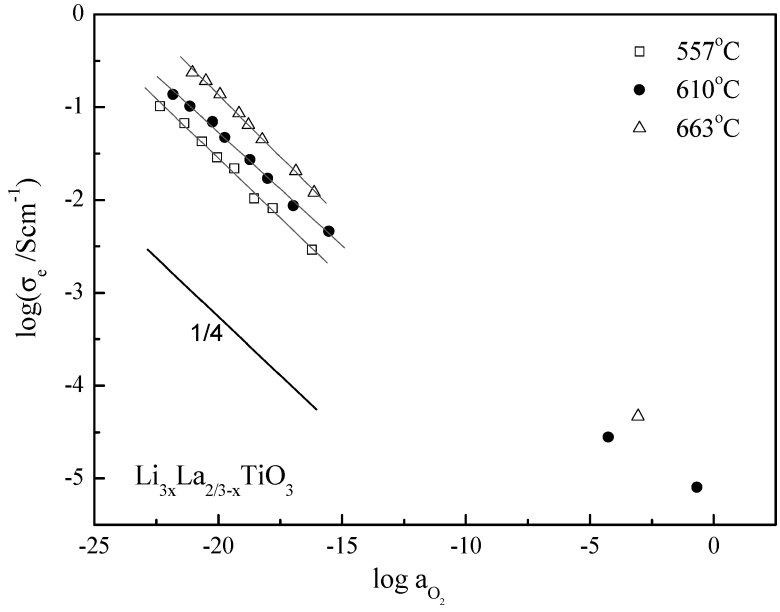

Fig. 5. Partial electronic conductivity of LLT vs. oxygen activity at different temperatures.

4.3. Partial Electronic Conductivity

The partial electronic conductivities as determined are shown against oxygen activity at different temperatures in Fig. 5. The electronic conductivity isotherms, $\sigma_e(T)$ may best be represented as

$$\sigma_e = \sigma_{e,o} a_{O_2}^{-1/4} \tag{18}$$

with $\sigma_{e,o} = (2.22 \pm 0.07) \times 10^{-7}$, $(5.43 \pm 0.13) \times 10^{-7}$, $(1.30 \pm 0.04) \times 10^{-6}$ Scm^{-1} at 557°, 610° and

663°C, respectively, rejecting the three data obtained in the oxidizing atmospheres ($\log a_{O_2} > -5$). It should be reminded that these three had to be evaluated by fitting only the partial transients that were considerably off from the steady sate because of the prohibitively sluggish polarization kinetics (see Fig. 3(a)) in these oxidizing atmospheres and hence, the fitted values for $\Delta V_{e,\infty}$ has to be subjected to a large uncertainty.

The electronic conductivity variation, Eq. (18) may be understood thermodynamically as follows: For a single phase system of LLT under a fixed pressure and temperature, the Gibbs-Duhem equation is written as

$$c_{Li}d\mu_{Li} + c_{La}d\mu_{La} + c_{Ti}d\mu_{Ti} + c_O d\mu_O = 0 \quad (19)$$

or in terms of oxide components ($LaO_{1.5}$ and TiO_2) neglecting oxygen nonstoichiometry

$$c_{Li}d\mu_{Li} + c_{La}d\mu_{LaO_{1.5}} + c_{Ti}d\mu_{TiO_2} + 0.5c_{Li}d\mu_O \approx 0 \quad (20)$$

where c_i denotes the concentration of chemical component i. If the concentrations of component La and Ti remain fixed due to their negligible mobility under isothermal isobaric condition, one may take $d\mu_{LaO_{1.5}} = d\mu_{TiO_2} = 0$ [18] and then,

$$d\mu_{Li} = d\mu_{Li^+} + d\mu_e \approx -\frac{1}{4}d\mu_{O_2} \quad (21)$$

Across the oxygen activity range in Fig. 5, the ionic conductivity remains essentially constant indicating that the irregular structure elements, say, $Li_i^{\bullet}$ and V_{La}''' are in the majority in a hypothetical ideal lattice $La_{2/3}TiO_3$. Therefore, $d\mu_{Li^+} \approx 0$ and it follows that

$$n \propto a_{O_2}^{-1/4} \quad (22)$$

However, the detailed defect mechanism leading to Eq. (22) is not immediately clear. It may involve the precipitation of a second phase like the redox equilibrium of donor-doped $BaTiO_3$ [29], but more systematic study is yet to be done.

4.4. *Ionic Transference Number*

In principle, the ionic transference number can be extracted from the polarization curves via Eq. (14) or (15), but the results are not sufficiently reliable as described earlier. So we have employed the total conductivity as measured by impedance spectroscopy [14] to evaluate the ionic transference number. The total conductivity of the present system in air is essentially the ionic conductivity and will remain unchanged over the a_{O_2} range examined. By combining these ionic conductivity values and the electronic conductivity of Eq. (18), the ionic transference number may best be estimated as

$$t_{Li^+} = \frac{\sigma_{Li^+}}{\sigma_{Li^+} + \sigma_{e,o}a_{O_2}^{-1/4}} \quad (23)$$

with $\sigma_{Li^+} = (4.84 \pm 0.01) \times 10^{-2}$, $(5.28 \pm 0.02) \times 10^{-2}$, $(5.37 \pm 0.02) \times 10^{-2}$ Scm^{-1} at 557°, 610° and 663°C, respectively. It is illustrated in Fig. 6. One can clearly recognize that the electrolytic domain (say, $t_{Li^+} \geq 0.99$) is limited to $\log a_{O_2} \geq -10.5$, -12.0, -13.0 at 663°, 610° and 557°C, respectively. According to Eq. (21), the electrolytic domain width of 1 down to, say, 10^{-12} of oxygen activity or $\Delta\log a_{O_2} = 12$ corresponds to a Li-activity difference of $\Delta\log a_{Li} = 3$. It means that when the Li activity difference imposed across an LLT electrolyte in a Li-battery is over 3 orders of magnitude at around 600°C, the electrolyte may likely fail due to electronic transference. So one has to further suppress the electronic transference if LLT is a choice of electrolyte even at room temperature. It is mentioned that by extrapolating the electrolytic domain width[2] from the three temperatures, one may expect the electrolytic domain to be $\log a_{O_2} \geq -52$. Taking the upper bound as air, then the electrolytic domain width in terms of Li-activity is $\Delta\log a_{Li} \approx 13$ at room temperature, which for a Li-battery, corresponds to an open-circuit voltage of only 0.8 V.

4.5. *Chemical Diffusivity*

The chemical diffusivities, corresponding to each of the electronic partial conductivity data in Fig. 5, were evaluated from the fitted parameter τ to the polarization processes according to Eq. (14) and shown in Fig. 7. It should be noted that, the relaxation times of the polarization and corresponding depolarization processes are in agreement with each other within the error bound. For example, the difference between the relaxation times evaluated from polarization (τ_p) and depolarization (τ_r) processes is less than 2% at 663°C in the oxygen activity of $\log a_{O_2} = -18.8$ (see Fig. 3(b)).

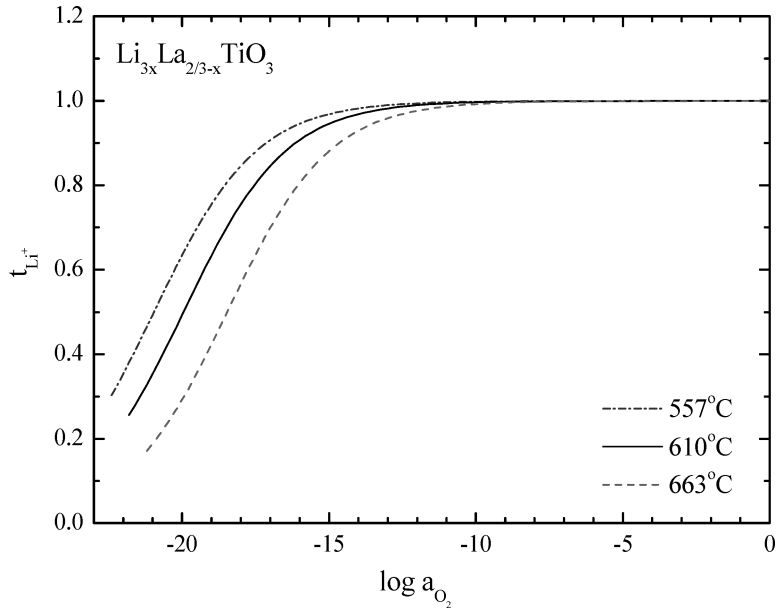

Fig. 6. Ionic transference number vs. oxygen activity at different temperatures.

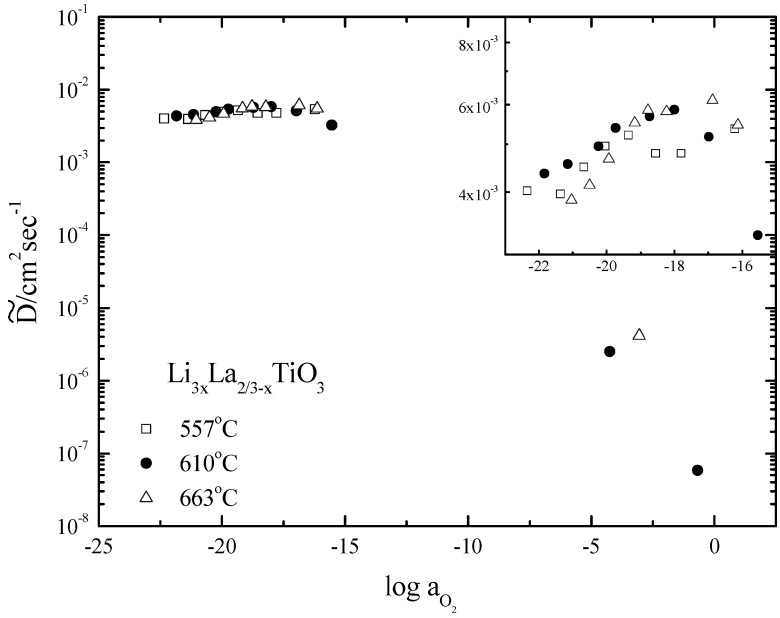

Fig. 7. Chemical diffusivity of LLT vs. oxygen activity at different temperatures. Inset: an enlarged view around the maximum chemical diffusivity. Fitting uncertainty of each datum is no greater than 3%.

It is seen that the magnitude of chemical diffusivity increases dramatically from, say, $\sim 10^{-8}$cm^2/s to $\sim 10^{-3}$cm^2/s as the oxygen activity reduces from 0.21 to far reducing atmospheres at all temperatures. The maximum value of $\tilde{D}$, 5.9×10^{-3} cm^2/s is quite comparable to that of the oxygen chemical diffusivity of perovskite $BaTiO_3$ [24, 28], $\sim 3 \times 10^{-3}$ cm^2/s. Furthermore, even though it is not so conspicuous as in $BaTiO_3$

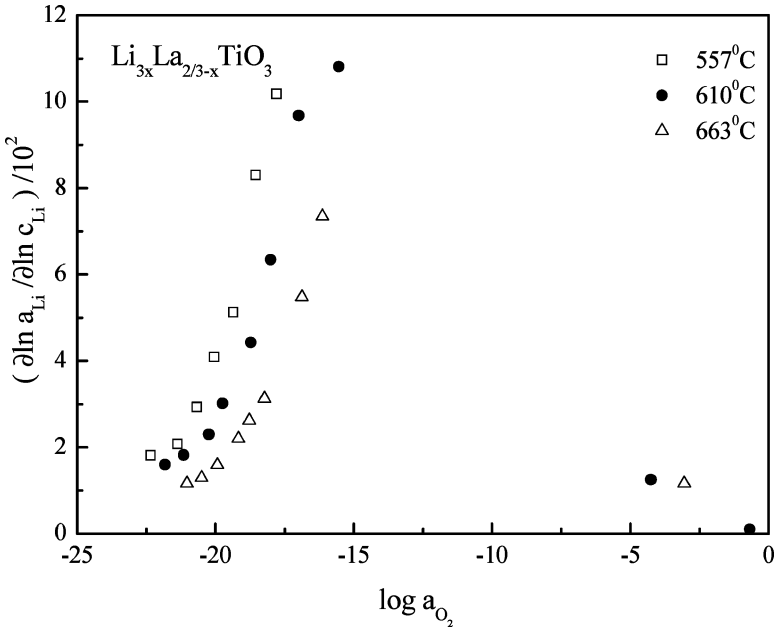

Fig. 8. Thermodynamic factor of LLT vs. oxygen activity at different temperatures.

[24, 28], the chemical diffusivity isotherms also exhibit a maximum at an oxygen activity of $\sim 10^{-17}$, see the inset in Fig. 7.

This sort of variation of the chemical diffusivity is attributed to the variation of the electronic transference number and thermodynamic factor combined [24, 28] (see Eq. (2)). As we now know the electronic transference number and ionic conductivity of the system, we can calculate the thermodynamic factor, $\partial \ln a_{\mathrm{Li}}/\partial \ln c_{\mathrm{Li}}$ via Eq. (2). The result is shown in Fig. 8. The thermodynamic factor takes the values on the order of 10–10^3.

It appears that the thermodynamic factor will show a maximum somewhere between log $a_{\mathrm{O}_2} = -15$ and -10. The thermodynamic factor becomes maximum normally at the stoichiometric composition, that is, $\delta = 0$ for, e.g., $Ag_{2+\delta}S$ [29] or $BaTiO_{3-\delta}$ [24]. It may, thus, be conjectured that the maximum corresponds to the stoichiometric composition, $Li_{3x}La_{2/3-x}TiO_3 (x = 0.13)$ for the present system, but it is yet to be confirmed.

5. Conclusions

As suspected, the LLT, $Li_{3x}La_{2/3-x}TiO_3$ becomes mixed-conductive as oxygen activity decreases. Particularly for the composition of $x = 0.13$, the partial electronic conductivity may be estimated as

$$\sigma_e = \sigma_{e,o} a_{\mathrm{O}_2}^{-1/4} \tag{24}$$

and hence, the ionic transference number as

$$t_{\mathrm{Li}^+} = \frac{\sigma_{\mathrm{Li}^+}}{\sigma_{\mathrm{Li}^+} + \sigma_{e,o} a_{\mathrm{O}_2}^{-1/4}} \tag{25}$$

with $\sigma_{\mathrm{Li}^+} = 0.048$, 0.053, 0.054 Scm^{-1} and $\sigma_{e,o} = 2.22 \times 10^{-7}$, 5.43×10^{-7}, 1.30×10^{-6} Scm^{-1} at 557°, 610° and 663°C, respectively. So one has to be warned that the LLT as a Li-electrolyte may easily turn mixed-conductive particularly under the anode condition.

With increasing electronic conductivity, the chemical diffusivity of Li also increases from $\sim 10^{-8}$ to $\sim 10^{-3}$ cm^2/s, exhibiting a maximum around $t_{\mathrm{Li}^+} \approx 0.8$. It is attributed to the variation of the thermodynamic factor ($\partial \ln a_{\mathrm{Li}}/\partial \ln c_{\mathrm{Li}}$) in association with the electronic transference number in accord with Wagner's theory of chemical diffusion. The thermodynamic factor is evaluated to be on the order of 10–10^3.

Acknowledgments

This work was partially supported by the Center for Advanced Materials Processing, Ministry of Science and Technology, Korea.

Notes

1. Conventionally, the polarization problem has been solved in terms of the conventional Fick's 2nd law *by assuming all the transport parameters, such as partial conductivities and the thermodynamic factor are constant in the given potentiostatic or galvanostatic condition*. Under the same assumptions, Fick's 2nd law can be written equivalently as Eq. (1) and one can again get the same results therefrom but with much less mathematical difficulty even for the potentiostatic polarization. Details are referred to Ref. [17].
2. One may estimate, from the data $\log a_{O_2} = -10.5, -12.0, -13.0$ at 663°, 610° and 557°C, respectively, the lower boundary of the electrolytic domain, where $t_{Li^+} = 0.99$, as $a_{O_2} = 7.2 \times 10^8 \cdot \exp(-3.6\ \text{eV/kT})$ in the temperature range examined. By extrapolating this equation, one can estimate the domain boundary at room temperature.

References

1. A.G. Belous, G.N. Novitskaya, S.V. Polyanetskaya, and Yu. I. Gornikov, *Izv. Akad, Nauk. SSSR, Neorg. Mater.*, **23**, 470 (1987).
2. Y. Inaguma, L. Chen, M. Itoh, T. Nakamura, T. Uchida, M. Ikuta, and M. Wakihara, *Solid State Commun*., **86**, 689 (1993).
3. Y. Inaguma, L. Chen, M. Itoh, and T. Nakamura, *Solid State Ionics*, **70–71**, 196 (1994).
4. M. Itoh, Y. Inaguma, W.H. Jung, L. Chen, and T. Nakamura, *Solid State Ionics*, **70–71**, 203 (1994).
5. Y. Inaguma, Y. Matsui, J. Yu, Y.J. Shan, T. Nakamura, and M. Itoh, *J. Phys. Chem. Solids*, **58**, 843 (1997).
6. K. Mizumoto and S. Hayashi, *Solid State Ionics*, **116**, 263 (1999).
7. G.X. Wang, P. Yao, D.H. Bradhurst, S.X. Dou, and H.K. Liu, *J. Mater. Sci*., **35**, 4289 (2000).
8. H. Kawai and J. Kuwano, *J. Electrochem. Soc*., **141**, L78 (1994).
9. Y. Inaguma and M. Itoh, *Solid State Ionics*, **86–88**, 257 (1996).
10. Y. Harada, T. Ishigaki, H. Kawai, and J. Kuwano, *Solid State Ionics*, **108**, 407 (1998).
11. Y. Harada,Y. Hirakoso, H. Kawai, and J. Kuwano, *Solid State Ionics*, **121**, 245 (1999).
12. O. Bohnke, C. Bohnke, and J.L. Fourquet, *Solid State Ionics*, **91**, 21 (1996).
13. A.K. Ivanov-Schitz, V.V. Kireev, and N.G. Chaban, *Solid State Ionics*, **136–137**, 501 (2000).
14. L.X. He and H.-I. Yoo, *Electrochim. Acta*, **48**, 1357 (2003).
15. M.H. Hebb, *J. Chem. Phys.*, **20**, 185 (1952).
16. C. Wagner, *Z. Elektrochem.*, **60**, 4 (1956).
17. K.-C. Lee and H.-I. Yoo, *J. Phys. Chem. Solids*, **60**, 911 (1999).
18. H.-I. Yoo, *Solid State Ionics*, **154–155**, 87 (2002).
19. I. Yokota, *J. Phys. Soc. Jap.*, **8**, 595 (1953).
20. I. Yokota, *J. Phys. Soc. Jap.*, **16**, 2213 (1961).
21. Weiss, *Z. Phys. Chem. NF*, **59**, 242 (1968).
22. J.M.S. Skakle, G.C. Mather, M. Morales, R.I. Smith, and A.R. West, *J. Mater. Chem.*, **5**, 1807 (1995).
23. C. Wagner, *Z. Phys. Chem. Abt.*, **B21**, 25 (1933).
24. C.-R. Song and H.-I. Yoo, *Phy. Rev. B*, **61**, 3975 (2000).
25. Y. Inaguma, T. Katsumata, M. Itoh, and Y. Morii, *J. Solid State Chem.*, **166**, 67 (2002).
26. O. Bohnke, J. Emery, J.L. Fourquet, and J.C. Badot, in *Recent Research Development in Solid State Ionics*, edited by S.G. Pandalai, (2003), Vol. 1, p. 47.
27. N.H. Chan, R.K. Sharma, and D.M. Smyth, *J. Am. Ceram. Soc*., **64**, 556 (1981).
28. C.-R. Song and H.-I. Yoo, *J. Am. Ceram. Soc*., **83**, 773 (2000).
29. K.D. Becker, H. Schmalzried, and V. Von Wurmb, *Solid State Ionics*, **11**, 213 (1983).